

ADSORPTION OF AMARANTH ONTO NATURAL PEANUT HUSK AND CATIONIC SURFACTANT-MODIFIED PEANUT HUSK FROM AQUEOUS SOLUTION: KINETIC, ISOTHERM AND THERMODYNAMIC ANALYSES

POLLOB GHOSH, SOMA SAHA, RATON KUMAR BISHWAS, SUBARNA KARMAKER and TAPAN KUMAR SAHA

Department of Chemistry, Jahangirnagar University, Savar, Dhaka 1342, Bangladesh

✉ *Corresponding author: Tapan Kumar Saha, tksaha_ju@yahoo.com*

Received October 10, 2021

Natural peanut husk (NPH) and hexadecyltrimethylammonium bromide (CTAB)-modified peanut husk (MPH) were used to study the adsorption characteristics of amaranth in aqueous solution. NPH and MPH were characterized by Fourier transform infrared (FTIR) spectroscopy. The pH_{zpc} values of NPH and MPH were estimated to be 5.06 and 5.96, respectively. The adsorption of amaranth onto both adsorbents was confirmed by the observations of field emission scanning electron microscopy (FE-SEM) and energy dispersive X-ray (EDX) analysis. Adsorption kinetic experiments were conducted at various contact time, solution pH, initial dye concentration, temperature, and ionic strength, respectively. Dye adsorption kinetics pursued the pseudo-second-order kinetic model. Adsorption isotherms obeyed the Langmuir model with the highest dye adsorption capacity of 20.88 $\mu\text{mol/g}$ for NPH at pH 2, and 117.65 $\mu\text{mol/g}$ for MPH at pH 4. The values of activation energy (E_a) for the adsorption process were determined to be 48.68 kJ/mol for NPH and 16.92 kJ/mol for MPH, respectively. Thermodynamic data confirmed that amaranth adsorption onto both adsorbents was an endothermic spontaneous physisorption process. The release of amaranth from dye-loaded adsorbents was performed in HCl solution (pH 1) and the recycled adsorbents were utilized six times without significant loss of their adsorption capacity.

Keywords: adsorption, kinetics, thermodynamics, biosorbent, surfactant modified biosorbent

INTRODUCTION

Dyeing industries release a huge amount of toxic effluents, mainly dyes, into natural water bodies, which causes severe threats to human beings and the aquatic life.^{1,2} It is very challenging to eliminate azo dyes from effluents because of their steady molecular structure. Therefore, the elimination of azo dyes from aqueous solution is a very important issue in our country, Bangladesh. The common methods presently engaged in removing dyes from wastewater include electrocoagulation and flocculation,³ ultrafiltration,⁴ oxidation,⁵ adsorption,⁶⁻⁹ membrane filtration,¹⁰ bacterial and enzymatic decolorization¹¹ etc. Among the mentioned techniques, adsorption is considered as an efficient and economical method, which is easy to operate for removing dyes from wastewater. Usually, activated carbon is used as an efficient adsorbent, as it has a large surface area and microporous configuration.¹² However,

activated carbon has been considered as a costly adsorbent because of its high production and regeneration costs. Therefore, researchers have been searching for low-cost adsorbents from naturally occurring raw materials. Our literature survey has shown that chitosan,⁷⁻⁹ various raw and modified agricultural wastes,¹³⁻²⁵ alumina reinforced polystyrene,²⁶ clay,²⁷ and fly ash²⁸ have been utilized to eliminate dyes from aqueous media. However, since the adsorption capacity of the mentioned adsorbents is insufficient, researchers are seeking for new adsorbents with better dye adsorption capacity.

Peanut (*Arachis hypogaea*) is an agricultural crop in tropical countries, such as Bangladesh. Peanut shell is an available agricultural by-product in our country. Proper application of a biosorbent must bring visible economic and social benefits, and turning a waste into a value-added product is expected to have such effects. Natural

and modified peanut husk has been used to eliminate organic molecules, such as crystal violet, methylene blue, tetracycline, light green, sunset yellow, fast green and indosol orange, and heavy metal ions, such as Pb(II), Cu(II) and Cr(III) from aqueous solution.^{16-18,21,24,29-32}

In the present study, natural peanut husk (NPH) and modified peanut husk (MPH) with hexadecyltrimethylammonium bromide (CTAB; Fig. 1a) were used to adsorb an anionic azo dye, amaranth (Fig. 1b), from aqueous solution. Both adsorbents were characterized by Fourier transform infrared (FTIR) spectroscopy. The adsorption of amaranth dye onto both adsorbents was confirmed by field emission electron microscopy (FE-SEM) and energy dispersive X-ray (EDX) spectroscopy. The effects of contact time, solution pH, amaranth dye concentration, ionic strength, and solution temperature on the dye adsorption kinetics were studied in batch experiments. The equilibrium adsorption of amaranth dye onto both adsorbents was examined in aqueous media at different temperatures. Batch adsorption kinetic data were evaluated by employing pseudo first-, second-order, Elovich and diffusion models, respectively. The validity of each kinetic model was verified by using a normalized standard deviation. The equilibrium adsorption data were examined by the Langmuir, Freundlich and Temkin isotherm models. The reusability of recycled adsorbents was evaluated. Thermodynamic parameters of the dye adsorption process were also discussed.

EXPERIMENTAL

Materials

The cationic surfactant hexadecyltrimethylammonium bromide (CTAB) and azo dye amaranth (Sigma–Aldrich, Germany) were used as received. The chemical structure of CTAB and amaranth are depicted in Figure 1. Other chemicals utilized in this experiment were in pure form.

Deionized water was produced by flowing distilled water across the deionizing column (Barnstead, Syboron Corporation, Boston, USA).

Preparation and characterization of NPH and MPH

Natural peanut husk (NPH) was gathered from the regional market of Savar, Dhaka, Bangladesh. Raw peanut husk was repeatedly cleaned with deionized water for removing dirt-like contamination and dried in open air. The dehydrated sample was powdered. To make it free from coloring materials, the powder of peanut husk was treated with petroleum ether for two days. Then, it was treated with warm deionized water (60 °C), next dried at 80 °C for 24 hours in an electric oven. The dried peanut husk was sieved using different meshes and the $\leq 75 \mu\text{m}$ particle sized peanut husk was preserved in the desiccator for use.

To prepare MPH, 5.0 g of peanut husk (particle size: $\leq 75 \mu\text{m}$) was transferred into a 500 mL beaker containing 250 mL of 0.5% (w/v) CTAB solution, and the mixture was agitated with a magnetic stirrer (120 rpm) at room temperature (30 °C) for 24 hours. After separating MPH from the mixture, it was repeatedly rinsed with deionized water to eliminate superficially held CTAB. Finally, MPH was desiccated at 80 °C overnight and preserved in an airtight glass bottle for further use.

The zero point charges (pH_{zpc}) of both adsorbents were determined by the pH drift method.¹³ A solution of 0.1 mol/L KCl was prepared and boiled to remove dissolved CO_2 and then cooled to room temperature. The initial pH of the KCl solution was adjusted between 2.0 and 12.0, by using 0.5 mol/L HCl or 0.5 mol/L NaOH. The adsorbent (0.1 g) was added into 25 mL of the pH-adjusted 0.1 mol/L KCl in a 125 mL reagent bottle. The bottles containing adsorbent samples were kept closed and equilibrated for 24 h. After 24 h, the final pH of each sample was measured and plotted against the initial pH. The pH at which the curve crosses the $\text{pH}_{\text{initial}} = \text{pH}_{\text{final}}$ line is taken as pH_{zpc} of NPH and MPH.

The Fourier transform infrared (FTIR) spectra of NPH and MPH were measured in KBr in the frequency range of 400–4000 cm^{-1} by employing an IRPrestige-21 FTIR Spectrophotometer (Shimadzu, Japan).

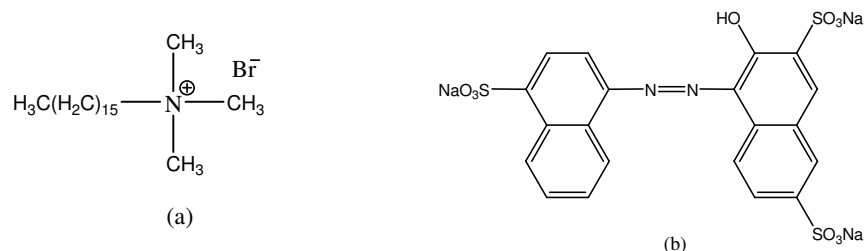


Figure 1: Structure of hexadecyltrimethylammonium bromide CTAB (a) and amaranth (b)

The surface morphology and elemental composition of both adsorbents were studied before and after dye adsorption by using field emission scanning electron microscopy (FE-SEM) and energy dispersive X-ray (EDX) analysis (JSM-7610F Schottky Field Emission Scanning Electron Microscope, JEOL Ltd., Japan).

Batch adsorption experiments

To evaluate the dye removal capacity of NPH and MPH, batch adsorption experiments were conducted in 125-mL stoppered bottles, which contained 0.1 g of adsorbent (NPH or MPH) and 25 mL of amaranth solution (30 $\mu\text{mol/L}$).⁸ Dye solution pH was maintained with 1 mol/L HCl or NaOH solution. The samples were shaken in a thermostated shaker at room temperature (30 ± 0.2 °C) until equilibrium. Every bottle was capped for avoiding evaporation of samples at high temperature. At expected time periods, sample bottles were withdrawn and centrifuged at 4000 rpm for 5 min. Amaranth concentration in the liquid phase was estimated by the spectrophotometric method using a Shimadzu UV-1900i spectrophotometer (Shimadzu, Japan), at λ_{max} : 521 nm (pH 1-10) and 502 nm (pH 11-12). The molar absorptivity of amaranth was determined to be 20.9×10^3 L/mol.cm at 521 nm and 13.0×10^3 L/mol.cm at 502 nm, respectively. The amount of amaranth dye adsorbed per unit adsorbent (NPH and MPH) at time t , q_t ($\mu\text{mol/g}$) was determined by Equation (1).⁸

$$q_t = \frac{V(C_0 - C_t)}{m} \quad (1)$$

where C_0 ($\mu\text{mol/L}$) is the initial concentration of amaranth and C_t ($\mu\text{mol/L}$) is the concentration of amaranth at time t ; V (L) is the volume of amaranth solution and m (g) is the amount of used adsorbents.

Dye adsorption kinetics was also analyzed at various concentrations of amaranth solution (30-200 $\mu\text{mol/L}$ for NPH and 30-1000 $\mu\text{mol/L}$ for MPH), ionic strengths using KCl solution (0.01-0.40 mol/L) and temperatures (30, 35, 40 and 45 °C), respectively. The equilibrium dye adsorption onto NPH and MPH were performed at various temperatures (30, 35, 40 and 45 °C) in aqueous solution (pH 2 for NPH and pH 4 for MPH) without KCl. The extent of amaranth dye adsorption on per unit adsorbents (NPH and MPH), q_e ($\mu\text{mol/g}$), at equilibrium, was computed by Equation (2).⁸

$$q_e = \frac{V(C_0 - C_e)}{m} \quad (2)$$

where C_e ($\mu\text{mol/L}$) is the equilibrium concentration of amaranth; C_0 , V and m have the same significance as mentioned earlier.

For the desorption experiment, HCl solution was used as an eluent. After the first adsorption, amaranth-loaded adsorbents were collected and dried at room temperature (30 °C) overnight. Amaranth-loaded

adsorbents (NPH and MPH) were shifted into 25 mL of 0.1 mol/L HCl (pH 1) solution and shaken for 60 min. Regenerated adsorbents were cleaned thoroughly with deionized water until the pH was neutral. The regenerated adsorbents were then dried at 100 °C, weighed and used again for the next adsorption experiment. The extent of adsorption and desorption was also estimated. All data exhibited in this study are the average of double measurements.

RESULTS AND DISCUSSION

Characterization of both adsorbents

The FTIR spectra of NPH and MPH are shown in Figure 2. It is observed that the FTIR spectrum of NPH (Fig. 2a) exhibited the typical vibration bands at 3420 cm^{-1} (broad) for N–H and O–H stretching, 2918 cm^{-1} for C–H stretching of CH_3 , 1734 cm^{-1} for amide-I (C=O group), 1616 cm^{-1} for amide-II (N-H bending), 1506 cm^{-1} for aromatic ring, 1373 cm^{-1} for $-\text{CH}_3$ bending, 1057 cm^{-1} for overlapping of C–O stretching and C–N stretching, and 759 cm^{-1} for N–H wagging. These bands are mainly responsible for the carbohydrates, lignin and cellulose, existing in peanut husk.³³ In the FTIR spectrum of MPH (Fig. 2b), the sharp peaks at 2920 and 2851 cm^{-1} were due to the C–H stretching of terminal $-\text{CH}_3$ and $-\text{CH}_2$ groups of the aliphatic surfactant tail, respectively. These results indicate that CTAB had been inserted into the surface of NPH. Moreover, other peak positions of MPH shifted slightly, which indicates that the main structure and composition of NPH remained intact after CTAB modification.³³ The addition of CTAB to NPH results in the formation of admicelles on the surface of the NPH particles, as noticed in CTAB modified cellulose noncrystals.³⁴ This is attributed to the hydrophobic attraction between the hydrophobic tails of the bound and free surfactant molecules.

The values of pH_{zpc} were computed to be 5.06 for NPH and 5.96 for MPH, respectively. The pH_{zpc} of hexadecylpyridinium bromide-modified peanut husk was reported to be 6.8.¹⁸ The results suggest that the surfaces of the adsorbents are positively charged at $\text{pH} < 5.06$ for NPH and $\text{pH} < 5.96$ for MPH, respectively, which is favorable for the adsorption of negatively charged dye molecules. In contrast, the surfaces of the adsorbents become negatively charged with increasing solution $\text{pH} > 5.06$ for NPH and > 5.96 for MPH, respectively, which is not suitable for adsorbing negatively charged dye molecules.

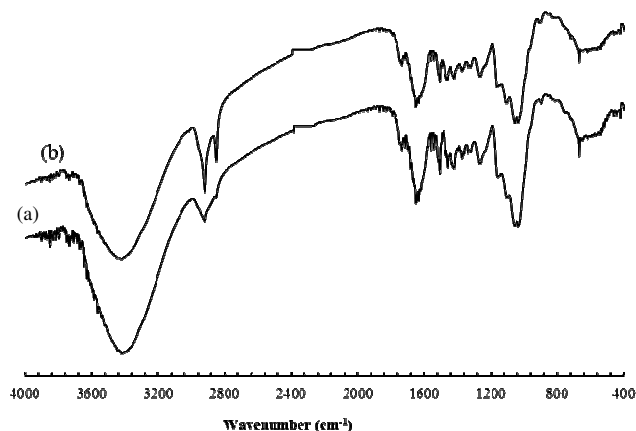


Figure 2: FTIR spectra of NPH (a) and MPH (b)

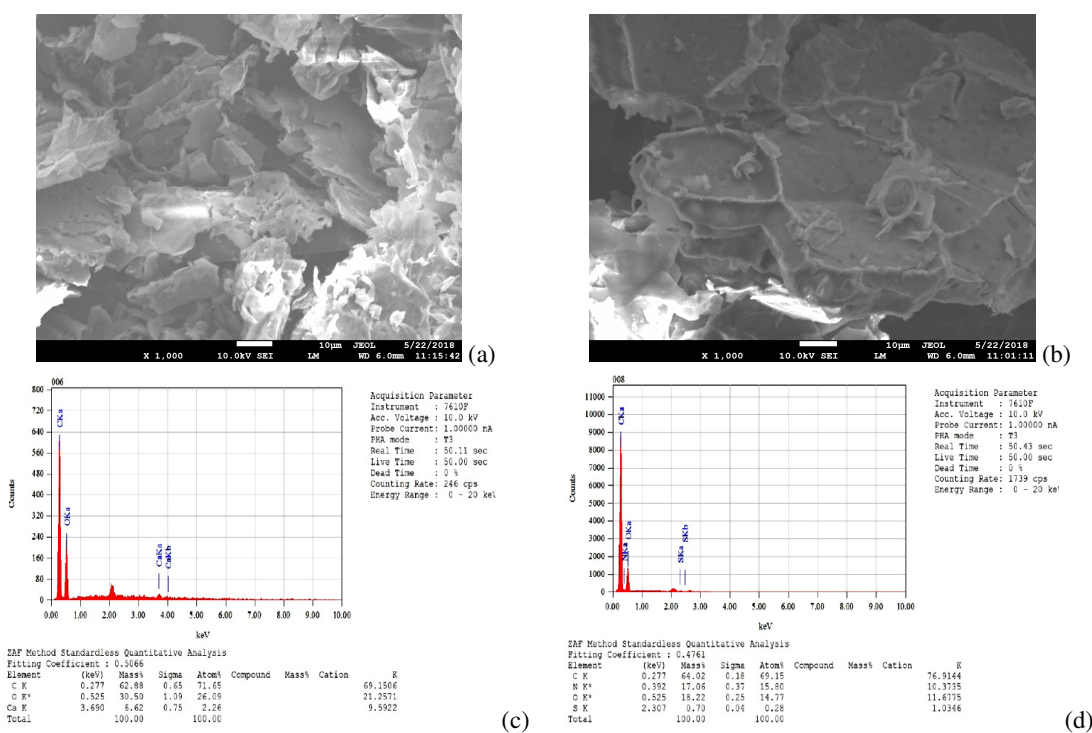


Figure 3: FE-SEM images and EDX data for NPH before (a, c) and after (b, d) amaranth dye adsorption

Confirmation of the adsorption of amaranth dye onto NPH and MPH by SEM and EDX

The surface morphologies of both adsorbents were investigated by using field emission scanning electron microscopy (FE-SEM), along with energy dispersive X-ray spectroscopy (EDX) at an accelerating voltage of 10 kV. Figure 3 shows the FE-SEM images and EDX data of NPH before and after amaranth adsorption. Before dye adsorption, it is noticed that the surface of NPH was rough and irregular (Fig. 3a), which is perhaps suitable for adsorption of dye molecules. The corresponding EDX data show that mainly

carbon and oxygen were present on the NPH surfaces (Fig. 3b). After dye adsorption, NPH surfaces became brighter and the pores were occupied (Fig. 3c). It is noticed that some particles had adhered onto the surface of NPH, which suggests the presence of amaranth molecules on the NPH surface.¹³ Moreover, the peaks of nitrogen and sulfur appeared in the EDX data of NPH (Fig. 3d) after amaranth adsorption. Therefore, it is confirmed that amaranth dye adsorption occurred on the surface of NPH.

Figure 4 shows the FE-SEM images and EDX data of MPH before and after amaranth dye

adsorption. It is noted that the FE-SEM image of MPH exhibited irregular and microporous surfaces before adsorption of amaranth (Fig. 4a). The corresponding elemental composition of fresh MPH is exhibited in Figure 4b. The elements of carbon, nitrogen, and oxygen were present on the surface of MPH. The surface brightness of MPH

increased after amaranth dye adsorption (Fig. 4c). It is noticed that the mass proportion of carbon and nitrogen increased on the surface of MPH after dye adsorption, and the existence of sulfur element was also noticed in Figure 4d. The results confirmed the adsorption of amaranth dye onto MPH.¹³

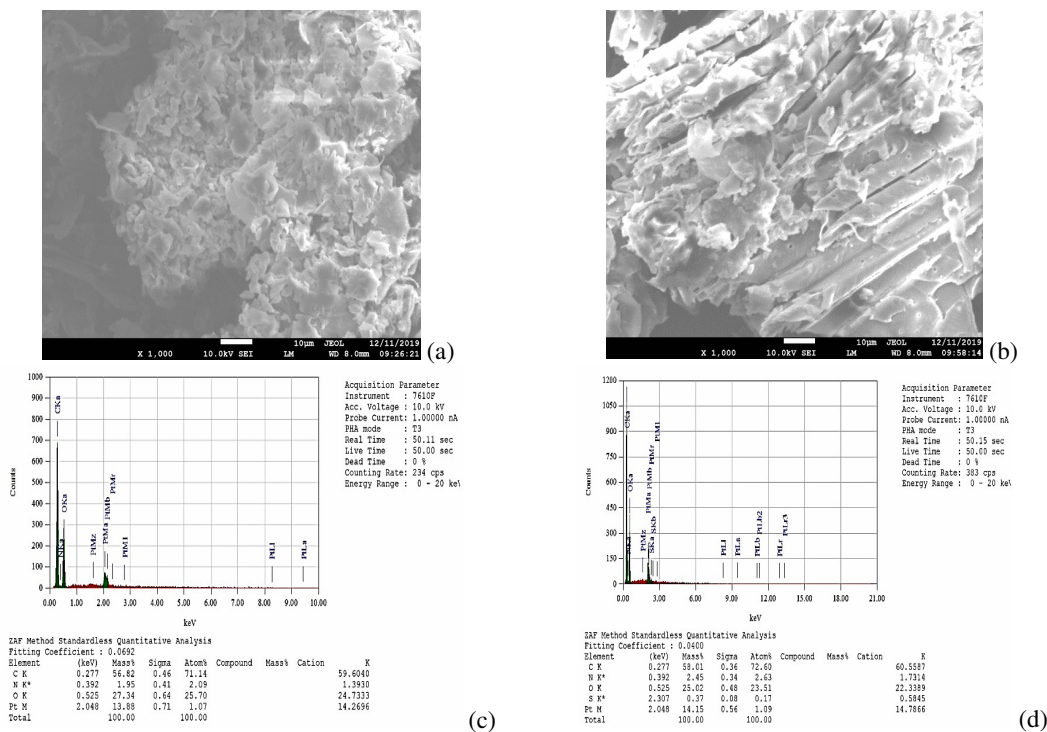


Figure 4: FE-SEM images and EDX data for MPH before (a, c) and after (b, d) amaranth dye adsorption

Effects of contact time

The impact of the interaction period on the adsorption of amaranth onto both adsorbents was examined in aqueous media (pH 2 for NPH and pH 4 for MPH) at 30 °C. The results are exhibited in Figure 5. Figures 5a and 5b represent the typical time resolved UV–visible absorption spectra of amaranth during adsorption onto NPH and MPH in aqueous medium, respectively. It is noted that the absorbance at 521 nm gradually decreased with increasing contact time. The results indicate that the dye adsorption onto both adsorbents gradually increased with time. The effects of the interaction period on the extent of amaranth dye adsorption (q_t) onto NPH and MPH are exhibited in Figure 5c. Dye was rapidly adsorbed onto both adsorbents (NPH and MPH) during the initial 5 min and then the adsorption rate decreased with time, ultimately achieving equilibrium within 20 min. However, data were taken for 60 min to establish the absolute

adsorption equilibrium. The initial adsorption rate was fast due to the adsorption of dye anions onto peripheral surfaces of the adsorbents (NPH and MPH). When the outer surfaces of adsorbents (NPH and MPH) were saturated with dye molecules, the rate of dye adsorption slowed down, and the dye molecules began to enter into the pores of the adsorbent particles with a slower rate.³⁵ Hence, the contact time of 60 min was kept constant as equilibrium time for the following studies.

Effects of solution pH

Solution pH significantly influences the adsorption of amaranth dye molecules onto NPH and MPH, because it controls the overall surface charges of both adsorbents and the ionization of dye molecules. In the present study, the amaranth dye adsorption kinetics was studied in aqueous media with varying pH: of 2–4 for NPH and 2–12 for MPH, with fixed dye concentration (30

$\mu\text{mol/L}$) and adsorbent dosage (0.1 g) for 60 min. The adsorption kinetics of amaranth dye at various solution pH values are depicted in Figure 6. The initial dye adsorption rate, h ($\mu\text{mol/g min}$), decreased significantly with increasing solution pH from 2 to 4, for NPH (Fig. 6a), while no dye adsorption occurred above pH 4 (Table 1). From Figure 6c, it is noted that the extent of equilibrium dye adsorption onto NPH, q_e ($\mu\text{mol/g}$), showed a similar pattern as observed for the initial rate of amaranth dye adsorption (Table 1). The highest capacity of amaranth dye adsorption onto NPH

was determined to be $7.46 \mu\text{mol/g}$ in aqueous medium at pH 2 (Fig. 6a). The pH_{zpc} of NPH was found to be 5.06. At pH 2, the surface of NPH became positively charged, which attracted the anionic dye molecules, hence, the adsorption rate and the extent of equilibrium dye adsorption became high. On the contrary, with rising the solution $\text{pH} > \text{pH}_{\text{zpc}}$, the surfaces of NPH particles turned to negative charges, causing electrostatic repulsion between NPH and amaranth dye molecules,^{8,13} which ultimately resulted in no adsorption of amaranth onto NPH at $\text{pH} > 4$.

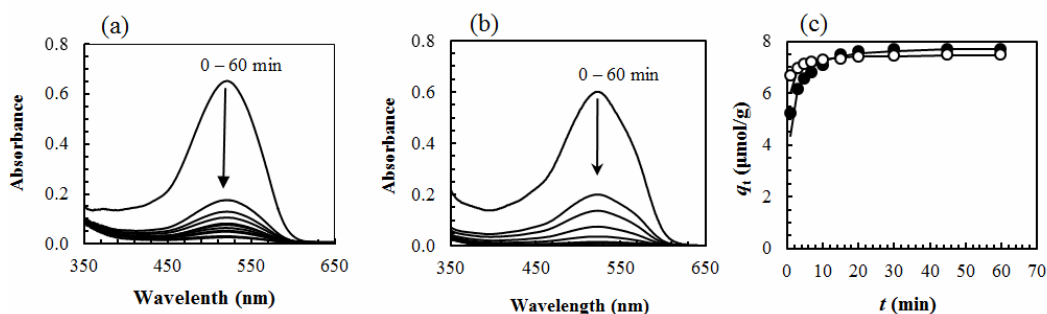


Figure 5: Typical time resolved UV-visible absorption spectra of amaranth taken at 1, 3, 5, 7, 10, 15, 20, 30, 45, and 60 min during adsorption onto NPH (a) and MPH (b) in aqueous solution; (c) Changes in extent of amaranth dye adsorption (q_t) onto NPH (\circ) and MPH (\bullet) with contact time (t); ([Amaranth]₀: $30 \mu\text{mol/L}$; solution volume: 25 mL; adsorbent dosage: 0.1 g; solution pH: 2 for NPH and 4 for MPH; temperature: 30°C)

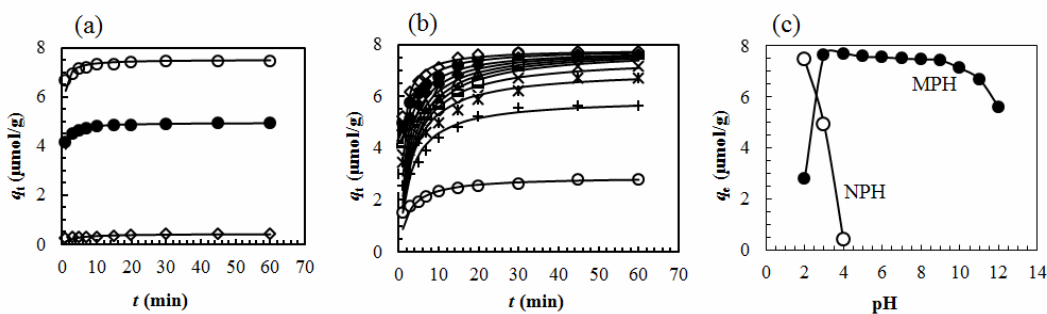


Figure 6: Changes in amount of amaranth dye adsorbed (q_t) onto NPH (a) and MPH (b) with contact time (t) at various solution pH values; ([Amaranth]₀: $30 \mu\text{mol/L}$; solution volume: 25 mL; adsorbent dosage: 0.1 g; temperature: 30°C ; solution pH: \circ : pH 2; \bullet : pH 3; \diamond : pH 4; \blacklozenge : pH 5; Δ : pH 6; \blacktriangle : pH 7; \square : pH 8; \blacksquare : pH 9; \times : pH 10; $*$: pH 11; $+$: pH 12); All solid lines were numerically mimicked by using Eq. (4) and the values of $q_{e(\text{cal})}$ and k_2 listed in Tables 1 and 2; (c) Effects of pH on the extent of equilibrium amaranth dye adsorption (q_e) onto NPH (\circ) and MPH (\bullet) from aqueous solution

In the case of MPH, the dye adsorption rate, h ($\mu\text{mol/g min}$), increased with rising solution pH up to 4 (Fig. 6b) and then it declined with rising solution pH 5-12 (Table 2). From Figure 6c, it is found that the extent of equilibrium dye adsorption, q_e ($\mu\text{mol/g}$), increased up to pH 3 and remained almost constant at pH 3-9. The values of q_e ($\mu\text{mol/g}$) gradually decreased with increasing

solution pH from 10 to 12 (Table 2). The highest amaranth adsorption onto MPH was obtained as $7.70 \mu\text{mol/g}$ at pH 4 (Fig. 6c). The pH_{zpc} of MPH was found to be 5.96. At pH 4, MPH surfaces became positively charged, which attracted anionic dye molecules, hence, the initial rate and the extent of equilibrium dye adsorption became high. On the contrary, with rising solution

$\text{pH} > \text{pH}_{\text{zpc}}$, the surfaces of MPH particles turned to negative charges, causing electrostatic repulsion between MPH and amaranth dye molecules,^{8,13} which ultimately results in less adsorption of amaranth onto MPH. Similar results were also noticed in adsorption of allura red AC onto hexadecylpyridinium bromide (CPB)-treated sawdust¹³ and light green anionic dye onto (CPB)-modified peanut husk¹⁸ in aqueous media. Therefore, all other kinetic experiments were conducted in aqueous media at pH 2 for NPH and pH 4 for MPH, respectively.

Effects of initial dye concentration

The changes in the amount of amaranth dye adsorbed (q_t) onto NPH (pH 2) and MPH (pH 4) with contact time (t) at various initial concentration of dye solutions and at the temperature of 30 °C are depicted in Figure 7. The initial rate, h ($\mu\text{mol/g}\cdot\text{min}$), increased with

increasing initial dye concentration in the solution (Tables 1 and 2), which indicates that the amaranth dye adsorption onto both adsorbents (NPH and MPH) was clearly dependent on dye concentration. With an increase in dye concentration from 30 to 200 $\mu\text{mol/L}$ for NPH and from 30 to 1000 $\mu\text{mol/L}$ for MPH, the amount of dye adsorbed at equilibrium (q_e) increased from 7.46 to 20.53 $\mu\text{mol/L}$ for NPH (Table 1) and from 7.70 to 114.29 $\mu\text{mol/g}$ for MPH (Table 2). The increase in dye concentration in the solution provides essential driving forces to overcome all mass transfer resistances between the adsorbate and the adsorbent, favoring adsorption.⁸ Analogous phenomena were also found in the adsorption of reactive blue 4 (RB4),⁷ remazol brilliant violet,⁸ and reactive black 5 (RB5)³⁶ onto chitosan in water.

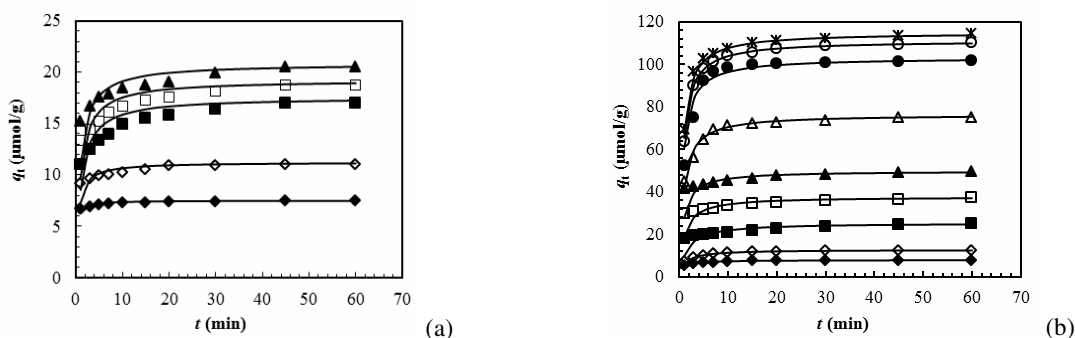


Figure 7: Changes in extent of amaranth dye adsorption (q_t) on NPH (a) and MPH (b) with contact time (t) at different dye concentrations; (solution volume: 25 mL; adsorbent dosage: 0.10 g; pH: 2 for NPH and 4 for MPH, temperature: 30 °C; $[\text{Amaranth}]_0$: \blacklozenge : 30 $\mu\text{mol/L}$; \diamond : 50 $\mu\text{mol/L}$; \blacksquare : 100 $\mu\text{mol/L}$; \square : 150 $\mu\text{mol/L}$; \blacktriangle : 200 $\mu\text{mol/L}$; \triangle : 300 $\mu\text{mol/L}$; \bullet : 500 $\mu\text{mol/L}$; \circ : 700 $\mu\text{mol/L}$; \square : 1000 $\mu\text{mol/L}$); All lines were numerically mimicked by using Eq. (4) and the values of $q_{e(\text{cal})}$ and k_2 recorded in Tables 1 and 2

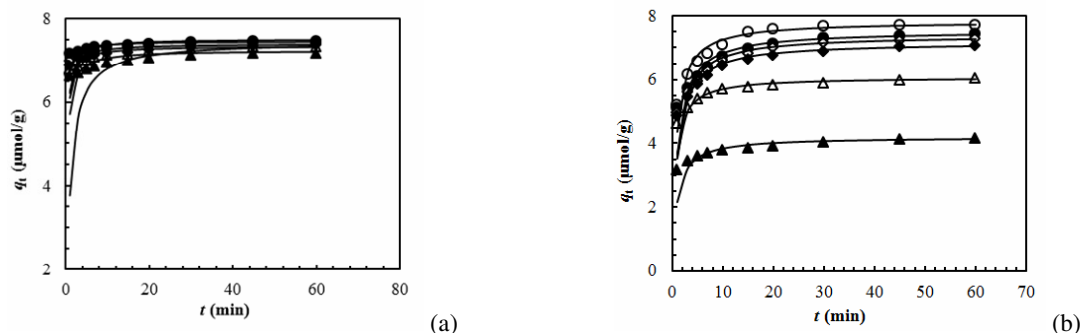


Figure 8: Changes in extent of amaranth dye adsorption (q_t) onto NPH (a) and MPH (b) with contact time (t) at various ionic strengths of the dye solution; ($[\text{Amaranth}]_0$: 30 $\mu\text{mol/L}$; solution volume: 25 mL; adsorbent dosage: 0.10 g; pH: 2 for NPH 4 for MPH; temperature: 30 °C; ionic strength: \circ : 0.0 mol/L; \bullet : 0.01 mol/L; \diamond : 0.05 mol/L; \blacklozenge : 0.10 mol/L; \triangle : 0.20 mol/L; \blacktriangle : 0.40 mol/L); All lines were mimicked by employing Eq. (4) and the values of $q_{e(\text{cal})}$ and k_2 recorded in Tables 1 and 2

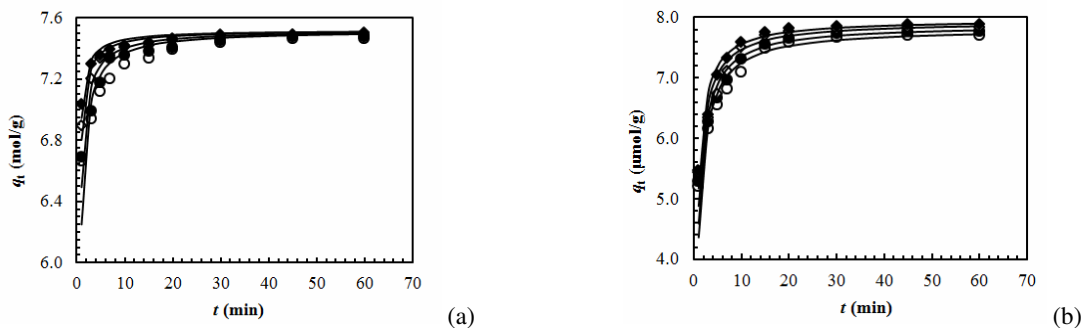


Figure 9: Changes in extent of amaranth dye adsorption (q_t) onto NPH (a) and MPH (b) with contact time (t) in aqueous media at various temperatures; ($[\text{Amaranth}]_0$: 30 $\mu\text{mol/L}$; solution volume: 25 mL; adsorbent dosage: 0.10 g; pH: 2 for NPH and 4 for MPH; Temperature: \circ : 30 $^\circ\text{C}$; \bullet : 35 $^\circ\text{C}$; \diamond : 40 $^\circ\text{C}$; \blacklozenge : 45 $^\circ\text{C}$); All lines were simulated by employing Eq. (4) and the values of $q_{e(\text{cal})}$ and k_2 recoded in Tables 1 and 2

Effects of ionic strength

The changes in the amount of amaranth dye adsorbed (q_t) onto NPH (pH 2) and MPH (pH 4) with contact time (t) in aqueous media was studied at various ionic strength, using a known amount of KCl in 30 $\mu\text{mol/L}$ amaranth solution at 30 $^\circ\text{C}$. The dye adsorption rate, h ($\mu\text{mol/g}\cdot\text{min}$), and the amount of dye adsorbed at equilibrium, q_e ($\mu\text{mol/g}$), onto both adsorbents (NPH and MPH) gradually declined with rising ionic strength of the dye solution (Fig. 8).

The results could be explained by a competitive effect between amaranth dye anions and Cl^- (from KCl) for the active sorption sites of NPH and MPH, as observed in the removal of reactive orange 13 (RO13) with jackfruit seed flakes²⁰ and reactive yellow 145 (RY145) with chitosan³⁷ from aqueous media, respectively. This also indicates the existence of electrostatic interactions between dye molecules and adsorbents.

Effects of temperature

The kinetics of amaranth dye adsorption on NPH (pH 2) and MPH (pH 4) was examined at various temperatures with a fixed 30 $\mu\text{mol/L}$ dye concentration for 60 min. The results are exhibited in Figure 9. It is found that the adsorption rate, h ($\mu\text{mol/g}\cdot\text{min}$), and the equilibrium adsorption, q_e ($\mu\text{mol/g}$), amplified with rising solution temperature from 30 to 45 $^\circ\text{C}$ (Tables 1 and 2), indicating an endothermic

process. The adsorption of amaranth dye molecules onto NPH and MPH occurred more efficiently at higher temperature due to the expansion of pore size or the creation of new active sites on the adsorbents,³⁸ as observed in the adsorption of amaranth onto pomegranate peel,¹⁹ RB4, RB5, and RY145 onto chitosan^{7,36,37} in aqueous solution, respectively.

Kinetic modeling

To know the adsorption kinetics and mechanism, the data received from batch adsorption experiments were analyzed by the pseudo-first-order,³⁹ pseudo-second-order,⁴⁰ Elovich,⁴¹ film diffusion⁴² and intraparticle diffusion⁴³ kinetic models. The pseudo-first-order kinetic model is expressed by Equation (3):³⁹

$$\log(q_e - q_t) = \log q_e - \frac{k_1}{2.0303} t \quad (3)$$

where k_1 (min^{-1}) is the pseudo-first-order sorption rate constant computed from the slope of a plot $\log(q_e - q_t)$ versus t .

The nonlinear form of the pseudo-second-order kinetic model is stated by Equation (4):⁴⁰

$$q_t = \frac{k_2 q_e^2 t}{(1 + k_2 q_e t)} \quad (4)$$

where k_2 ($\text{g}/\mu\text{mol}\cdot\text{min}$) is the rate constant of the pseudo-second-order adsorption obtained from Equation (5):

$$\frac{t}{q_t} = \frac{1}{k_2 q_e^2} + \frac{1}{q_e} t \quad (5)$$

Table 1
Kinetic parameters derived from different kinetic models employed for amaranth dye adsorption on NPH from aqueous media

Parameters	$q_{e(\text{exp})}$ ($\mu\text{mol/g}$)	Pseudo-first-order kinetics				Pseudo-second-order kinetics					Elovich kinetics				
		$q_{e(\text{cal})}$ ($\mu\text{mol/g}$)	k_1 (min^{-1})	R^2	Δq_e (%)	$q_{e(\text{cal})}$ ($\mu\text{mol/g}$)	k_2 ($\text{g}/\mu\text{mol min}$)	h ($\mu\text{mol/g min}$)	R^2	Δq_e (%)	$q_{e(\text{cal})}$ ($\mu\text{mol/g}$)	α ($\mu\text{mol/g min}$)	β ($\text{g}/\mu\text{mol}$)	R^2	Δq_e (%)
Solution pH; particle size: $\leq 75 \mu\text{m}$; $[\text{Dye}]_0$: $30 \mu\text{mol/L}$; Temp. $30 \text{ }^\circ\text{C}$															
2	7.46	0.67	0.114	0.978	11.64	7.49	0.657	36.900	1.000	0.77	7.57	1.33×10^{14}	5.05	0.937	1.49
3	4.92	0.48	0.087	0.885	14.28	4.94	0.736	18.018	1.000	0.96	5.03	4.19×10^{09}	5.56	0.895	2.25
4	0.41	0.20	0.065	0.959	37.26	0.43	0.840	0.156	0.992	11.50	0.41	2.74×10^{00}	19.60	0.942	3.76
$[\text{Dye}]_0$ ($\mu\text{mol/L}$); solution pH 2; particle size: $\leq 75 \mu\text{m}$; Temp. $30 \text{ }^\circ\text{C}$															
50	11.04	2.07	0.106	0.966	9.04	11.14	0.165	20.533	0.999	0.95	11.23	2.78×10^{07}	1.95	0.971	1.32
100	16.96	5.29	0.076	0.975	6.71	17.24	0.056	16.666	0.999	1.04	17.49	1.89×10^{03}	0.64	0.988	1.43
150	18.75	5.06	0.074	0.978	6.58	18.97	0.054	19.723	0.999	0.83	19.28	1.45×10^{04}	0.69	0.985	1.30
200	20.53	4.70	0.067	0.960	6.46	20.74	0.053	23.094	0.999	0.74	20.90	1.17×10^{05}	0.74	0.992	0.98
Temp. ($^\circ\text{C}$); solution pH 2, particle size: $\leq 75 \mu\text{m}$; $[\text{Dye}]_0$: $30 \mu\text{mol/L}$															
35	7.47	0.53	0.108	0.904	11.76	7.49	0.827	46.511	1.000	0.63	7.60	1.32×10^{15}	5.34	0.874	1.61
40	7.49	0.33	0.100	0.878	11.91	7.50	1.269	71.428	1.000	0.45	7.58	2.24×10^{22}	7.60	0.839	1.31
45	7.50	0.30	0.110	0.948	11.93	7.50	1.507	88.495	1.000	0.00	7.56	4.99×10^{29}	9.89	0.850	1.09
Ionic strength (mol/L); solution pH 2; particle size: $\leq 75 \mu\text{m}$; $[\text{Dye}]_0$: $30 \mu\text{mol/L}$; Temp. $30 \text{ }^\circ\text{C}$															
0.01	7.44	0.25	0.081	0.978	12.01	7.45	1.374	76.335	1.000	0.45	7.46	3.76×10^{42}	14.04	0.971	0.67
0.05	7.41	0.35	0.101	0.931	11.95	7.42	1.168	64.516	1.000	0.45	7.48	3.34×10^{26}	9.01	0.940	1.16
0.10	7.36	0.43	0.067	0.965	11.92	7.37	0.686	37.313	1.000	0.45	7.39	5.42×10^{23}	8.24	0.987	0.72
0.20	7.31	0.55	0.090	0.981	11.86	7.34	0.644	34.722	1.000	0.79	7.37	1.25×10^{19}	6.78	0.966	1.13
0.40	7.17	0.58	0.076	0.996	11.93	7.19	0.518	26.881	0.999	0.66	7.20	4.21×10^{17}	6.46	0.976	0.86

Table 2
Kinetic parameters derived from different kinetic models employed for amaranth dye adsorption on MPH in aqueous media

Parameters	$q_{e(\text{exp})}$ ($\mu\text{mol/g}$)	Pseudo first-order kinetics				Pseudo second-order kinetics					Elovich kinetics				
		$q_{e(\text{cal})}$ ($\mu\text{mol/g}$)	k_1 (min^{-1})	R^2	Δq_e (%)	$q_{e(\text{cal})}$ ($\mu\text{mol/g}$)	k_2 ($\text{g}/\mu\text{mol min}$)	h ($\mu\text{mol/g min}$)	R^2	Δq_e (%)	$q_{e(\text{cal})}$ ($\mu\text{mol/g}$)	α ($\mu\text{mol/g min}$)	β ($\text{g}/\mu\text{mol}$)	R^2	Δq_e (%)
Solution pH; particle size: $\leq 75 \mu\text{m}$; $[\text{Dye}]_0$: $30 \mu\text{mol/L}$; Temp. $30 \text{ }^\circ\text{C}$															
2	3.00	1.19	0.070	0.952	14.95	2.89	0.152	1.271	0.999	3.69	2.87	2.22×10^{01}	2.88	0.980	4.08
3	7.65	3.64	0.165	0.975	8.73	7.83	0.107	6.587	0.999	1.85	7.96	8.21×10^{02}	1.40	0.967	2.42
4	7.70	2.47	0.147	0.991	9.90	7.82	0.161	9.862	0.999	1.50	8.06	3.87×10^{03}	1.59	0.932	2.61
5	7.58	3.42	0.112	0.992	8.97	7.81	0.078	4.726	0.999	2.11	7.84	2.23×10^{02}	1.24	0.969	2.22
6	7.56	3.92	0.104	0.966	8.41	7.85	0.058	3.580	0.998	2.37	7.73	9.21×10^{01}	1.13	0.962	1.84
7	7.51	4.77	0.109	0.923	7.35	7.85	0.048	2.952	0.997	2.59	7.62	5.08×10^{01}	1.06	0.955	1.49
8	7.48	4.23	0.084	0.962	8.03	7.85	0.041	2.524	0.996	2.71	7.52	3.51×10^{01}	1.02	0.954	0.91
9	7.44	3.87	0.063	0.992	8.47	7.82	0.036	2.227	0.995	2.76	7.40	2.90×10^{01}	1.01	0.953	0.92
10	7.13	3.76	0.067	0.991	8.58	7.50	0.039	2.223	0.996	2.84	7.08	2.86×10^{01}	1.06	0.957	1.03
11	6.70	3.37	0.065	0.994	9.08	7.02	0.045	2.212	0.997	2.81	6.73	2.65×10^{01}	1.11	0.969	0.93
12	5.61	4.11	0.127	0.982	7.28	5.92	0.058	2.031	0.999	3.31	5.90	1.22×10^{01}	1.14	0.959	3.20
$[\text{Dye}]_0$ ($\mu\text{mol/L}$); solution pH 4; particle size: $\leq 75 \mu\text{m}$; Temp. $30 \text{ }^\circ\text{C}$															
50	12.50	3.99	0.087	0.938	7.78	12.67	0.063	10.173	0.999	1.10	13.05	5.63×10^{02}	0.78	0.943	1.98
100	24.99	6.89	0.051	0.994	5.67	25.32	0.024	15.649	0.998	0.77	24.73	3.08×10^{04}	0.56	0.969	0.68
150	37.37	7.53	0.053	0.968	4.87	37.59	0.026	35.971	0.999	0.42	36.71	3.12×10^{06}	0.50	0.975	0.73
200	49.52	8.11	0.058	0.974	4.33	49.75	0.025	62.500	0.999	0.32	49.62	2.97×10^{08}	0.46	0.975	0.22
300	74.99	18.13	0.100	0.848	3.35	76.34	0.016	90.909	1.000	0.52	79.90	8.59×10^{03}	0.14	0.862	0.99
500	101.79	22.01	0.123	0.772	2.92	103.09	0.014	147.059	0.999	0.37	111.44	4.20×10^{03}	0.09	0.763	1.02
700	110.12	25.47	0.105	0.891	2.79	111.11	0.013	158.730	1.000	0.30	116.60	1.93×10^{04}	0.10	0.812	0.77
1000	114.29	22.92	0.094	0.848	2.79	114.94	0.013	169.492	1.000	0.24	116.05	5.30×10^{04}	0.11	0.805	0.39
Temp. ($^\circ\text{C}$); solution pH 4, particle size: $\leq 75 \mu\text{m}$; $[\text{Dye}]_0$: $30 \mu\text{mol/L}$															
35	7.77	7.80	0.023	0.991	0.74	7.88	0.177	11.013	0.999	1.42	7.99	5.75×10^{03}	1.63	0.918	2.00
40	7.83	7.96	0.022	0.990	1.53	7.94	0.202	12.690	0.999	1.41	8.25	8.83×10^{03}	1.66	0.897	2.74
45	7.88	8.02	0.022	0.990	1.58	7.97	0.232	14.749	1.000	1.27	8.03	1.39×10^{04}	1.71	0.864	1.61
Ionic strength (mol/L); solution pH 4; particle size: $\leq 75 \mu\text{m}$; $[\text{Dye}]_0$: $30 \mu\text{mol/L}$; Temp. $30 \text{ }^\circ\text{C}$															
0.01	7.42	2.25	0.103	0.995	10.21	7.54	0.127	7.199	0.999	1.56	3.49	3.28×10^{03}	1.66	0.972	8.91
0.05	7.29	2.16	0.098	0.987	10.36	7.39	0.128	6.974	0.999	1.45	7.50	2.57×10^{03}	1.66	0.970	2.10
0.10	7.07	1.83	0.082	0.939	10.79	7.17	0.135	6.930	0.999	1.49	7.67	3.74×10^{03}	1.77	0.968	3.65
0.20	6.05	1.02	0.069	0.855	12.36	6.12	0.169	6.329	0.999	1.46	6.17	5.04×10^{05}	2.97	0.944	1.88
0.40	4.17	1.19	0.062	0.956	13.80	4.19	0.252	4.444	0.999	1.13	4.19	1.11×10^{05}	4.09	0.996	1.01

The values of k_2 and q_e were computed from the intercept and the slope of the plot $\frac{t}{q_t}$ versus t . The initial dye adsorption rate, h ($\mu\text{mol/g}\cdot\text{min}$), was calculated by Equation (6):⁴⁰

$$h = k_2 q_e^2 \quad (6)$$

The Elovich kinetic model is stated by Equation (7):⁴¹

$$q_t = \frac{1}{\beta} \ln(\alpha\beta) + \frac{1}{\beta} \ln t \quad (7)$$

where α ($\mu\text{mol/g}\cdot\text{min}$) denotes the initial dye adsorption rate and β ($\text{g}/\mu\text{mol}$) is related to the extent of surface coverage and the activation energy of chemisorption. The Elovich constants were obtained from the plot of q_t versus $\ln t$.

The significance and validity of each model can be verified using a normalized standard deviation (Δq_e , %),⁴⁴ which can be determined as follows:

$$\Delta q_e (\%) = 100 \sqrt{\frac{\sum [(q_{e,\text{exp}} - q_{e,\text{cal}})/q_{e,\text{exp}}]^2}{N-1}} \quad (8)$$

where N is the number of data points, $q_{e,\text{exp}}$ ($\mu\text{mol/g}$) and $q_{e,\text{cal}}$ ($\mu\text{mol/g}$) are the experimental and calculated equilibrium dye adsorption capacity.

The kinetic parameters, along with correlation coefficients (R^2) and normalized standard deviation (Δq_e , %), found for different kinetic models, are shown in Table 1 for NPH and in Table 2 for MPH. The R^2 values attained from the pseudo-first-order (≤ 0.994) and the Elovich (≤ 0.980) kinetic models were insignificant, compared to the values obtained from the pseudo-second-order (≥ 0.999) kinetic model (Tables 1 and 2). The Δq_e (%) values attained from the pseudo-second-order kinetic model were significantly smaller than those obtained from the pseudo-first-order and the Elovich kinetic models (Tables 1 and 2). In addition, the values of $q_{e(\text{cal})}$ computed from the pseudo-second-order kinetic model and the observed values of $q_{e(\text{exp})}$ are analogous (Tables 1 and 2) to those noticed in the removal of RB5 and RY145 with chitosan from aqueous solution.^{36,37} Hence, the adsorption of amaranth dye onto NPH and MPH from aqueous solution follows pseudo-second-order adsorption kinetics.

The film diffusion model is denoted by Equation (9):

$$\ln(1-F) = -k_{fd}t \quad (9)$$

$$F = \frac{q_t}{q_e} \quad (10)$$

where k_{fd} (1/min) is the rate constant of film diffusion and F is the fractional attainment of equilibrium. The film diffusion rate constant was computed from the plot of $\ln(1-F)$ versus t . The values of k_{fd} and R^2 are shown in Tables 3 and 4.

The intraparticle diffusion model is denoted by Equation (11):⁴³

$$q_t = k_{id}t^{0.5} + I \quad (11)$$

where k_{id} ($\mu\text{mol/g}\cdot\text{min}^{0.5}$) represents the intraparticle diffusion rate constant and I ($\mu\text{mol/g}$) signifies the intercept. Figure 10 shows the characteristic plots of q_t versus $t^{0.5}$ at different initial dye concentrations. There were two linear portions in each plot, which suggests that two phenomena occurred during the dye adsorption process. The first is rapid exterior surface diffusion of the adsorbent, with a rate constant k_{id1} ($\mu\text{mol/g}\cdot\text{min}^{1/2}$), and the second is slow interior surface diffusion of the adsorbent, with a rate constant k_{id2} ($\mu\text{mol/g}\cdot\text{min}^{1/2}$).³⁷ The values of k_{id1} ($\mu\text{mol/g}\cdot\text{min}^{1/2}$) and k_{id2} ($\mu\text{mol/g}\cdot\text{min}^{1/2}$) presented in Tables 3 and 4 were determined from the slope of corresponding straight lines in q_t versus $t^{0.5}$ plots. It is noted that none of the straight lines passed across the origin (Fig. 10), which suggests that the mechanism of the present dye adsorption is multifaceted. The surface adsorption and intraparticle diffusion mechanisms might be responsible for the amaranth dye adsorption process, as noticed in RY145 adsorption onto chitosan from aqueous solution.³⁷

Activation parameters

The k_2 values noted in Tables 1 and 2 at various temperatures were employed to determine the activation energy (E_a) for amaranth dye adsorption on NPH and MPH from aqueous media. The relationship among the E_a , rate constant (k_2) and temperature (T) can be stated by Equation (12):⁴⁵

$$\ln k_2 = -\frac{E_a}{RT} + \text{constant} \quad (12)$$

where R (8.314 J/mol K) is the gas constant. E_a was estimated to be 48.68 kJ/mol for NPH and 19.62 kJ/mol for MPH from the slopes of plots $\ln k_2$ versus $1/T$ ($R^2 = 0.982$ for NPH and $R^2 = 0.990$ for MPH). The E_a values were determined to be 25.52 kJ/mol for remazol brilliant violet adsorption onto chitosan,⁸ 25.40 kJ/mol for RO13 adsorption onto jackfruit seed flakes²⁰ and 19.72 kJ/mol for the adsorption of RY145 dye on chitosan.³⁷ The value of E_a reflects the nature of the adsorption process. Usually, the activation

energy is 5-40 kJ/mol for the physisorption process and 40-800 kJ/mol for the chemisorption process.⁴⁶ Hence, the E_a (48.68 kJ/mol for NPH and 19.62 kJ/mol for MPH) values indicate that the amaranth dye adsorption onto both adsorbents is a physisorption process.

The following Equations (13) and (14) were applied to determine the changes in the enthalpy of activation (ΔH^\ddagger), entropy of activation (ΔS^\ddagger), and Gibbs free energy of activation (ΔG^\ddagger) for the present adsorption system:^{47,48}

$$\ln\left(\frac{k_2}{T}\right) = -\frac{\Delta H^\ddagger}{RT} + \ln\frac{k_B}{h_p} + \frac{\Delta S^\ddagger}{R} \quad (13)$$

$$\Delta G^\ddagger = \Delta H^\ddagger - T\Delta S^\ddagger \quad (14)$$

where k_2 (g/mol min), R and T remain constant, as explained earlier, h_p is the Plank constant (h_p : 6.626×10^{-34} Js) and k_B is the Boltzman constant (k_B : 1.381×10^{-23} J/K). The values of ΔH^\ddagger and ΔS^\ddagger were determined from the slope and y-intercept of the plot $\ln(k_2/T)$ versus $1/T$ ($R^2 = 0.980$ for NPH and $R^2 = 0.987$ for MPH). The values of ΔH^\ddagger were calculated to be 46.10 kJ/mol for NPH and 16.96 kJ/mol for MPH, indicating an endothermic adsorption with weak interaction between amaranth and both adsorbents.⁴⁹ The ΔS^\ddagger values (18.29 J/mol K for NPH and -89.49 J/mol K for MPH) suggest that the amaranth anions

were more organized at the activated state and interface rather than in the bulk solution phase for MPH.⁴⁹ Analogous results were found in the elimination of reactive red 239 (RR239) dye with chitosan 8B from aqueous media.⁵⁰ The ΔG^\ddagger values were computed as 40.46, 40.55, 40.46 and 40.37 kJ/mol for NPH and 44.08, 44.53, 44.97 and 45.42 kJ/mol for MPH at 30, 35, 40 and 45 °C, respectively. The positive ΔG^\ddagger values indicate the presence of an energy barrier in the adsorption process.^{37,50}

Adsorption isotherm

Various isotherm models were applied to analyze equilibrium adsorption data for understanding the interaction between the adsorbate and the adsorbent. The plots of q_e versus C_e at different solution temperatures are depicted in Figure 11. The present adsorption was found to be an endothermic process as the extent of equilibrium dye adsorption (q_e ; $\mu\text{mol/g}$) onto both adsorbents enhanced with rising solution temperature from 30 to 45 °C. Freundlich,⁵¹ Temkin⁵² and Langmuir⁵³ isotherm models were utilized to interpret equilibrium adsorption data found at various temperatures.

Table 3
Values of diffusion rate constants for amaranth dye adsorption onto NPH

Parameters	Film diffusion model		Intra-particle diffusion model			
	k_{fd} (min^{-1})	R^2	k_{id1} ($\mu\text{mol/g}\cdot\text{min}^{1/2}$)	R^2	k_{id2} ($\mu\text{mol/g}\cdot\text{min}^{1/2}$)	R^2
Solution pH; particle size: $\leq 75 \mu\text{m}$; $[\text{Dye}]_0$: 30 $\mu\text{mol/L}$, Temp. 30 °C						
2	0.113	0.977	0.295	0.973	0.032	0.819
3	0.087	0.883	0.294	0.920	0.029	0.941
4	0.065	0.958	0.032	0.966	0.023	0.895
[Dye] ₀ ($\mu\text{mol/L}$); solution pH 4; particle size: $\leq 75 \mu\text{m}$; Temp. 30 °C						
50	0.106	0.967	0.488	0.958	0.113	0.695
100	0.076	0.975	1.772	0.996	0.412	0.934
150	0.073	0.979	1.555	0.993	0.413	0.934
200	0.067	0.960	1.504	0.968	0.500	0.914
Temp. (°C); solution pH 4, particle size: $\leq 75 \mu\text{m}$; $[\text{Dye}]_0$: 30 $\mu\text{mol/L}$						
35	0.108	0.903	0.324	0.952	0.025	0.885
40	0.100	0.878	0.233	0.881	0.017	0.852
45	0.113	0.951	0.170	0.848	0.013	0.823
Ionic strength (mol/L); solution pH 4; particle size: $\leq 75 \mu\text{m}$; $[\text{Dye}]_0$: 30 $\mu\text{mol/L}$; Temp. 30 °C						
0.01	0.070	0.927	0.083	0.971	0.018	0.910
0.05	0.088	0.928	0.161	0.982	0.017	0.856
0.10	0.057	0.923	0.136	0.935	0.042	0.909
0.20	0.076	0.916	0.172	0.962	0.041	0.840
0.40	0.065	0.931	0.146	0.987	0.050	0.904

Table 4
Values of diffusion rate constants for amaranth dye adsorption onto MPH

Parameters	Film diffusion model		Intra-particle diffusion model			
	k_{fd} (min^{-1})	R^2	k_{id1} ($\mu\text{mol/g}\cdot\text{min}^{1/2}$)	R^2	k_{id2} ($\mu\text{mol/g}\cdot\text{min}^{1/2}$)	R^2
Solution pH; particle size: $\leq 75 \mu\text{m}$; $[\text{Dye}]_0$: $30 \mu\text{mol/L}$; Temp. $30 \text{ }^\circ\text{C}$						
2	0.070	0.952	0.379	0.995	0.094	0.947
3	0.155	0.975	0.805	0.984	0.112	0.703
4	0.147	0.993	0.865	0.959	0.053	0.813
5	0.112	0.993	0.849	0.991	0.185	0.772
6	0.104	0.967	0.814	0.974	0.258	0.823
7	0.109	0.924	0.763	0.983	0.319	0.796
8	0.084	0.962	0.725	0.995	0.378	0.850
9	0.063	0.992	0.708	0.992	0.433	0.921
10	0.067	0.991	0.691	0.994	0.388	0.912
11	0.065	0.994	0.728	0.992	0.326	0.926
12	0.127	0.982	0.859	0.986	0.188	0.749
[Dye] $_0$ ($\mu\text{mol/L}$); solution pH 4; particle size: $\leq 75 \mu\text{m}$; Temp. $30 \text{ }^\circ\text{C}$						
50	0.087	0.937	1.857	0.954	0.213	0.969
100	0.051	0.994	1.357	0.995	0.844	0.978
150	0.053	0.968	1.724	0.990	0.736	0.994
200	0.058	0.974	1.746	0.998	0.757	0.977
300	0.100	0.848	12.590	0.957	0.811	0.946
500	0.123	0.772	22.177	0.908	0.480	0.979
700	0.105	0.891	18.292	0.859	1.071	0.925
1000	0.094	0.848	16.934	0.822	1.029	0.982
Temp. ($^\circ\text{C}$); solution pH 4, particle size: $\leq 75 \mu\text{m}$; [Dye] $_0$: $30 \mu\text{mol/L}$						
35	0.146	0.988	0.918	0.971	0.051	0.793
40	0.154	0.944	0.942	0.988	0.031	0.813
45	0.150	0.936	1.006	0.966	0.031	0.813
Ionic strength (mol/L); solution pH 4; particle size: $\leq 75 \mu\text{m}$; [Dye] $_0$: $30 \mu\text{mol/L}$; Temp. $30 \text{ }^\circ\text{C}$						
0.01	0.103	0.995	0.736	0.996	0.113	0.872
0.05	0.098	0.987	0.759	0.995	0.112	0.881
0.10	0.082	0.940	0.741	0.997	0.112	0.968
0.20	0.069	0.855	0.504	0.971	0.070	0.999
0.40	0.062	0.956	0.286	0.971	0.080	0.984

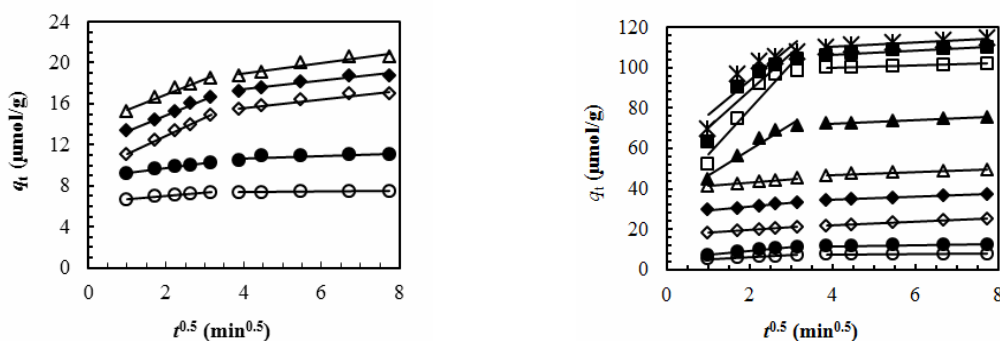


Figure 10: Characteristic plots of q_t versus $t^{0.5}$ for amaranth dye adsorption on MPH (a) and MPH (b) at various initial concentration of solutions (solution volume: 25 mL ; adsorbent dosage: 0.10 g ; temperature: $30 \text{ }^\circ\text{C}$; pH: 2 for MPH and 4 for MPH; [Amaranth] $_0$: \circ : $30 \mu\text{mol/L}$; \bullet : $50 \mu\text{mol/L}$; \diamond : $100 \mu\text{mol/L}$; \blacklozenge : $150 \mu\text{mol/L}$; Δ : $200 \mu\text{mol/L}$; \blacktriangle : $300 \mu\text{mol/L}$; \square : $500 \mu\text{mol/L}$; \blacksquare : $700 \mu\text{mol/L}$; \square : $1000 \mu\text{mol/L}$)

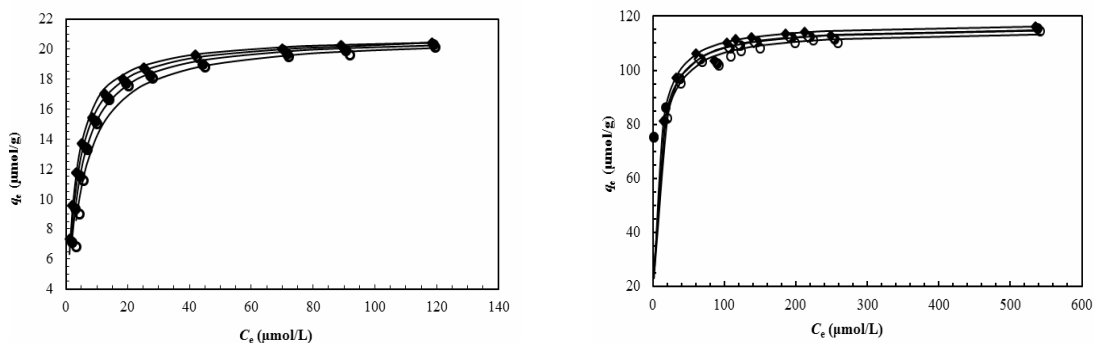


Figure 11: Adsorption isotherm of amaranth onto NPH (a) and MPH (b) at different temperatures ([Amaranth]₀: 10-200 μmol/L for NPH and 30-1000 μmol/L for MPH; solution volume: 25 mL; adsorbent dosage: 0.10 g; Temperature: ○: 30 °C; ●: 35 °C; ◇: 40 °C; ◆: 45 °C); All lines were mimicked by employing Langmuir isotherm Eq. (20) and the values of a_L and K_L at different temperatures listed in Tables 5 and 6

The equations of the applied isotherm models are given below:

Freundlich model:

$$\text{Nonlinear form } q_e = K_F C_e^{\frac{1}{n}} \quad (15)$$

$$\text{Linear form } \ln q_e = \frac{1}{n} \ln C_e + \ln K_F \quad (16)$$

Temkin model:

$$\text{Nonlinear form } q_e = \frac{RT}{b} \ln(K_T C_e) \quad (17)$$

$$\text{Linear form } q_e = \frac{RT}{b} \ln K_T + \frac{RT}{b} \ln C_e \quad (18)$$

Langmuir model:

$$\text{Nonlinear form } q_e = \frac{K_L C_e}{(1 + a_L C_e)} \quad (19)$$

$$\text{Linear form } \frac{C_e}{q_e} = \frac{1}{K_L} + \frac{a_L}{K_L} C_e \quad (20)$$

where C_e (μmol/L), q_e (μmol/g), R (8.314 J/mol K) and T (K) have the same meaning as described earlier, K_F ((μmol/g)(μmol/L)^{-1/n}) and n are Freundlich isotherm constants, showing the ability and strength of the adsorption, respectively. K_T (μmol/L) is the Temkin isotherm constant, b (J/mol) relates to the heat of adsorption, K_L (L/g) denotes the Langmuir constant and a_L (L/μmol) is the Langmuir binding constant. The highest dye adsorption onto both adsorbents, q_m (μmol/g), was determined from the ratio of K_L/a_L . Tables 5 and 6 illustrate the values of the isotherm parameters. All equilibrium adsorption isotherm data were explained more satisfactorily by the Langmuir isotherm model rather than by the Freundlich and Temkin isotherm models, due to the highest correlation coefficients (R^2) (Tables 5 and 6).^{7,13}

Table 5

Values of various isotherm constants and thermodynamic parameters for amaranth dye adsorption on NPH in aqueous media (pH 2)

Isotherm/ thermodynamics	Parameters	Temperature (°C)			
		30	35	40	45
Freundlich model	K_F ((μmol/g)(μmol/L) ^{-1/n})	7.13	7.90	8.39	8.87
	N	4.03	4.42	4.63	4.88
	R^2	0.780	0.842	0.861	0.880
Temkin model	K_T (μmol/L)	5.31	9.27	13.05	19.32
	b (J/mol)	0.747	0.823	0.869	0.927
	R^2	0.871	0.918	0.928	0.941
Langmuir model	K_L (L/g)	4.44	5.62	6.81	7.94
	a_L (L/μmol)	0.213	0.269	0.326	0.380
	q_m (μmol/g)	20.86	20.89	20.89	20.90
	R^2	0.999	0.999	1.000	0.999
Thermodynamics	ΔG (kJ/mol)	-30.84	-31.86	-32.88	-33.90
	ΔH (kJ/mol)		30.97		
	ΔS (J/mol.K)		20.40		
	R^2		0.993		

Table 6
Values of various isotherm constants and thermodynamic parameters for amaranth dye adsorption on MPH in aqueous media (pH 4)

Isotherm/ thermodynamics	Parameters	Temperature (°C)			
		30	35	40	45
Freundlich model	$K_F ((\mu\text{mol/g})(\mu\text{mol/L})^{-1/n})$	68.51	69.54	69.23	70.69
	n	11.44	11.34	11.20	11.38
	R^2	0.935	0.954	0.924	0.910
Temkin model	$K_T (\mu\text{mol/L})$	3.04×10^3	2.93×10^3	2.68×10^3	3.64×10^3
	$b (\text{J/mol})$	308.60	307.01	309.52	317.47
	R^2	0.935	0.956	0.927	0.912
Langmuir model	$K_L (\text{L/g})$	14.47	15.67	16.29	17.61
	$a_L (\text{L}/\mu\text{mol})$	0.126	0.135	0.140	0.150
	$q_m (\mu\text{mol/g})$	113.64	114.94	116.28	117.65
	R^2	0.999	0.999	0.999	0.999
Thermodynamics	$\Delta G (\text{kJ/mol})$	-29.58	-30.25	-30.84	-31.50
	$\Delta H (\text{kJ/mol})$		8.92		
	$\Delta S (\text{J/mol.K})$		127.09		
	R^2		0.989		

The values of q_m were found to be 20.86 $\mu\text{mol/g}$ at 30 °C and 20.90 $\mu\text{mol/g}$ at 45 °C for NPH, and 113.64 $\mu\text{mol/g}$ at 30 °C and 117.65 $\mu\text{mol/g}$ at 45 °C for MPH, respectively.

Comparison of amaranth dye adsorption onto various adsorbents

The amount of amaranth dye adsorbed (q_m) onto NPH and MPH was compared with those obtained for other adsorbents, as described in the literature (Table 7). It is found that MPH adsorbed a larger amount of amaranth dye, compared with other adsorbents, such as peanut hull,²¹ tamarind pod shells,²² bottom-ash and de-oiled soya,²³ alumina reinforced polystyrene,²⁶ and smectite clay,²⁷ respectively. Hence, both adsorbents (NPH and MPH) could possibly be used as eco-friendly biosorbents to eliminate amaranth dye from aqueous solution.

Thermodynamics

Thermodynamic analysis of the adsorption process is essential to inspect the spontaneity of the system. The changes in Gibbs free energy (ΔG , kJ/mol), enthalpy (ΔH , kJ/mol) and entropy (ΔS , J/mol K) were estimated by using the following equations:⁵⁴

$$\Delta G = -RT \ln a_L \quad (21)$$

$$\ln a_L = \frac{\Delta S}{R} - \frac{\Delta H}{RT} \quad (22)$$

where a_L (L/mol), R (8.314 J/mol K) and T (K) have the same meaning as described earlier. The slope and y-intercept of the plot $\ln a_L$ versus $1/T$ ($R^2 = 0.993$ for NPH and $R^2 = 0.989$ for MPH) were used to calculate the values of ΔH : 30.97 kJ/mol, ΔS : 20.40 J/mol for NPH (Table 5) and ΔH : 8.92 kJ/mol, ΔS : 127.09 J/mol for MPH (Table 6), respectively. ΔH values indicate that the dye adsorption was an endothermic process. ΔS values confirmed the existence of randomness at the solid-liquid interface.⁵⁰ Negative values of ΔG : -30.84 to -33.90 kJ/mol for NPH (Table 5) and -29.58 to -31.50 kJ/mol for MPH (Table 6), respectively, confirm the viability and spontaneous nature of the amaranth dye adsorption onto both adsorbents.

Reuse of NPH and MPH

A recyclable adsorbent is very important for the industry, to achieve an economic wastewater remedy plant.¹⁸ Figure 12 shows the reusability of NPH and MPH for adsorption of amaranth dye from aqueous solution. In the direct adsorption step, 30 $\mu\text{mol/L}$ dye solution (pH 2 for NPH and 4 for MPH) was agitated with 0.1 g adsorbent (NPH and MPH) for 60 min at 30 °C. The values of q_c were determined to be 7.46 $\mu\text{mol/g}$ for NPH and 7.70 $\mu\text{mol/g}$ for MPH. The dye release from amaranth-loaded NPH and MPH was studied in 0.1 mol/L HCl (pH 1) for 240 min at 30 °C.

Table 7
Comparison of adsorption capacities of various adsorbents for the removal of amaranth from aqueous media

Adsorbent	Particle size (μm)	pH	Temperature ($^{\circ}\text{C}$)	q_m ($\mu\text{mol/g}$)	Reference
Natural peanut husk (NPH)	≤ 75	2	30	20.86	This study
CTAB-modified peanut husk (MPH)	≤ 75	4	30	113.64	This study
Peanut hull	150 – 180	2	20	24.65	21
Tamarind pod shells	---	2	---	107.59	22
Bottom ash	≤ 300	2	30	11.58	23
De-oiled soya	≤ 300	2	30	46.32	23
Alumina reinforced polystyrene	150 -300	2	30	13.69	26
Smectite clay	8	2	---	3.05	27

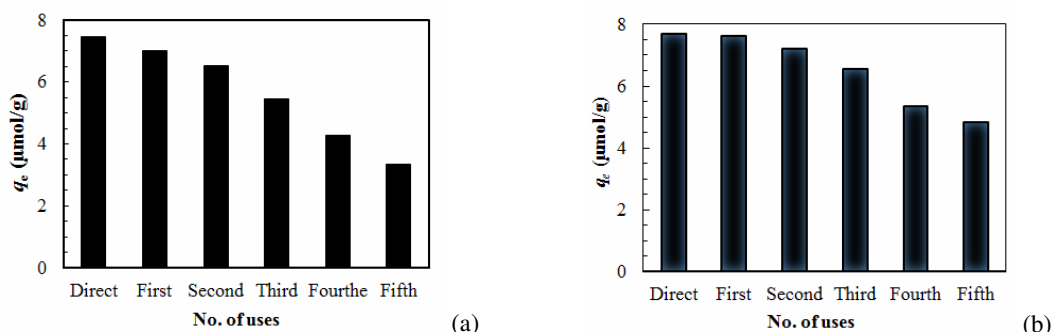


Figure 12: Values of q_e ($\mu\text{mol/g}$) observed in various adsorption steps of amaranth onto NPH (a) and MPH (b) in aqueous solution at 30°C (dye concentration: $30\ \mu\text{mol/L}$; solution volume: $25\ \text{mL}$; adsorbent dosage: $0.1\ \text{g}$ and pH: 2 for NPH and 4 for MPH)

In the desorption step, the release rate of dye was rapid during the first 15 min and 99% amaranth dye was discharged from the amaranth-loaded adsorbents within 240 min (figure not shown). It suggests that the protonated amaranth dye molecules were easily liberated from the dye-loaded adsorbents in strongly acidic solution (pH 1). In the first reuse adsorption step, recycled NPH and MPH were used to adsorb $30\ \mu\text{mol/L}$ dye solution (pH 2 for NPH and pH 4 for MPH) for 60 min. A similar amount of dye adsorbed was noticed as that in the direct step. The values of q_e were found to be 7.46, 7.02, 6.52, 5.44, 4.26 and $3.34\ \mu\text{mol/g}$ for NPH and 7.70, 7.62, 7.21, 6.54, 5.36 and $4.84\ \mu\text{mol/g}$ for MPH in the direct use, first, second, third, fourth and fifth reuse steps, respectively. These results indicate that both NPH and MPH can be used as eco-friendly adsorbents for removing amaranth from aqueous media effectively.

CONCLUSION

In this study, natural peanut husk (NPH) and hexadecyltrimethylammonium bromide-treated peanut husk (MPH) were employed for removing

amaranth dye from aqueous media. NPH and MPH were characterized by FTIR and the pH_{zpc} values were found to be 5.06 for NPH and 5.96 for MPH, respectively. The results obtained by field emission scanning electron microscopy (FE-SEM) and energy dispersive X-ray (EDX) spectroscopy confirmed the adsorption of amaranth dye onto NPH and MPH. The dye adsorption capacities of both adsorbents increased with rising contact time, dye concentration and temperature, respectively, and decreased with rising solution ionic strengths. The maximum dye adsorption occurred in aqueous media at pH 2 for NPH and pH 4 for MPH. The batch adsorption kinetics agreed very well with the pseudo-second-order kinetic model, whereas intra-particle diffusion played an important role in the rate-limiting step. Equilibrium dye adsorption isotherms followed the Langmuir model rather than the Freundlich and Temkin models. The highest dye adsorption capacities were found to be $20.86\ \mu\text{mol/g}$ at 30°C and $20.90\ \mu\text{mol/g}$ at 45°C for NPH, and $113.64\ \mu\text{mol/g}$ at 30°C and $117.65\ \mu\text{mol/g}$ at 45°C for MPH, respectively. The values of activation energy (E_a): $48.68\ \text{kJ/mol}$

for NPH and 19.62 kJ/mol for MPH) and thermodynamic parameters (ΔH : 30.97 kJ/mol, ΔS : 20.40 J/mol K, ΔG : -30.84 to -33.90 kJ/mol for NPH and ΔH : 8.92 kJ/mol, ΔS : 127.09 J/mol K, ΔG : -29.58 to -31.50 kJ/mol for MPH) show that the dye adsorption process is spontaneous, endothermic, guided by the physiosorption mechanism. The dye-loaded adsorbents released amaranth in 0.1 mol/L HCl solution (pH 1) and the recycled NPH and MPH were reused 5-6 times in dye adsorption. The present work confirms that both NPH and MPH may be employed as effective biosorbents to remove amaranth dye from aqueous solution.

ACKNOWLEDGEMENTS: We thankfully acknowledge the support given by Jahangirnagar University, the Ministry of Science and Technology, Government of People's Republic of Bangladesh and Alexander von Humboldt Foundation (Ref. 3.4-8151/Saha (GA-Nr. 20 007)), Germany.

REFERENCES

- ¹ B. Lellis, C. Z. Favaro-Polonio, J. A. Pamphile and J. C. Polonio, *Biotechnol. Res. Innov.*, **3**, 275 (2019), <https://doi.org/10.1016/j.biori.2019.09.001>
- ² M. Berradi, R. Hsissou, M. Khudhair, M. Assouag, O. Cherkaoui *et al.*, *Heliyon*, **5**, e02711 (2019), <https://doi.org/10.1016/j.heliyon.2019.e02711>
- ³ A. Olad, A. R. Amani-Ghadim, M. S. S. Dorraji and M. H. Rasoulifard, *Clean-Soil, Air, Water*, **38**, 401 (2010), <https://doi.org/10.1002/clen.200900213>
- ⁴ H. Metivier-Pignon, C. Faur-Brasquet and P. L. Cloirec, *Sep. Purif. Technol.*, **31**, 3 (2003), [https://doi.org/10.1016/S1383-5866\(02\)00147-8](https://doi.org/10.1016/S1383-5866(02)00147-8)
- ⁵ T. K. Saha, H. Frauendorf, M. John, S. Dechert and F. Meyer, *ChemCatChem*, **5**, 796 (2013), <https://doi.org/10.1002/cctc.201200475>
- ⁶ M. C. Stanciu and M. Nichifor, *Colloid Polym. Sci.*, **297**, 45 (2019), <https://doi.org/10.1007/s00396-018-4439-z>
- ⁷ S. Karmaker, A. J. Nag and T. K. Saha, *Russ. J. Phys. Chem. A*, **94**, 2349 (2020), <https://doi.org/10.1134/S0036024420110126>
- ⁸ S. Karmaker, A. J. Nag and T. K. Saha, *Cellulose Chem. Technol.*, **53**, 373 (2019), <https://doi.org/10.35812/CelluloseChemTechnol.2019.53.38>
- ⁹ T. K. Saha, S. Karmaker, H. Ichikawa and Y. Fukumori, *J. Colloid Interface Sci.*, **286**, 433 (2005), <https://doi.org/10.1016/j.jcis.2005.01.037>
- ¹⁰ C. Thamaraiselvan and M. Noel, *Crit. Rev. Environ. Sci. Technol.*, **45**, 1007 (2015), <https://doi.org/10.1080/10643389.2014.900242>
- ¹¹ S. Mishra and A. Maiti, *Environ. Sci. Pollut. Res.*, **25**, 8286 (2018), <https://doi.org/10.1007/s11356-018-1273-2>
- ¹² T. D. Martins, D. Schimmel, J. B. O. das Santos and E. A. da Silva, *J. Chem. Eng. Data*, **58**, 106 (2013), <https://doi.org/10.1021/je300946j>
- ¹³ T. K. Saha, R. K. Bishwas, S. Karmaker and Z. Islam, *ACS Omega*, **5**, 13358 (2020), <https://doi.org/10.1021/acsomega.0c01493>
- ¹⁴ R. A. Fideles, G. M. D. Ferreira, F. S. Teodoro, O. F. H. Adarme, L. H. M. Silva *et al.*, *J. Colloid Interface Sci.*, **515**, 172 (2018), <https://doi.org/10.1016/j.jcis.2018.01.025>
- ¹⁵ X. Ren, X. Zhang, L. Zhang and R. Han, *Desalin. Water Treat.*, **51**, 4514 (2013), <https://doi.org/10.1080/19443994.2012.741776>
- ¹⁶ J. Liu, Z. Wang, H. Li, C. Hu, P. Raymer *et al.*, *Bioresour. Technol.*, **249**, 307 (2018), <https://doi.org/10.1016/j.biortech.2017.10.010>
- ¹⁷ M. T. Islam, A. H. M. G. Hyder, R. S. Arana, C. Hernandez, T. Guinto *et al.*, *J. Environ. Chem. Eng.*, **7**, 102816 (2019), <https://doi.org/10.1016/j.jece.2018.102816>
- ¹⁸ B. Zhao, W. Xiao, Y. Shang, H. Zhu and R. Han, *Arab. J. Chem.*, **10**, S3595 (2017), <https://doi.org/10.1016/j.arabjc.2014.03.010>
- ¹⁹ H. A. Ali, H. K. Egzar, N. M. Kamal, N. Abdulsahab and M. S. Mashkour, *Int. J. Basic Appl. Sci.*, **13**, 57 (2013), http://ijens.org/Vol_13_I_04/133404-9595-IJBAS-IJENS.pdf
- ²⁰ S. Karmaker, M. N. Uddin, H. Ichikawa, Y. Fukumori and T. K. Saha, *J. Environ. Chem. Eng.*, **3**, 583 (2015), <https://doi.org/10.1016/j.jece.2014.09.010>
- ²¹ R. Gong, Y. Ding, M. Li, C. Yang, H. Liu *et al.*, *Dyes Pigm.*, **64**, 187 (2005), <https://doi.org/10.1016/j.dyepig.2004.05.005>
- ²² N. Ahalya, M. N. Chandraprabha, R. D. Kanamadi and T. V. Ramachandra, *J. Biochem. Technol.*, **3**, S189 (2012)
- ²³ A. Mittal, L. Kurup (Krishnan) and V. K. Gupta, *J. Hazard. Mater.*, **117**, 171 (2005), <https://doi.org/10.1016/j.jhazmat.2004.09.016>
- ²⁴ S. Sadaf and H. N. Bhatti, *Clean Technol. Environ.*, **16**, 527 (2014), <https://doi.org/10.1007/s10098-013-0653-z>
- ²⁵ E. Dovi, A. N. Kani, A. A. Aryee, M. Jie, J. Li *et al.*, *Environ. Sci. Pollut. Res.*, **28**, 28732 (2021), <https://doi.org/10.1007/s11356-021-12550-4>
- ²⁶ R. Ahmad and R. Kumar, *Clean-Soil, Air, Water*, **39**, 74 (2011), <https://doi.org/10.1002/clen.201000125>
- ²⁷ L. T. Nanganoa, J. M. Ketcha and J. N. Ndi, *Res. J. Chem. Sci.*, **4**, 7 (2014), <http://www.isca.in/rjcs/Archives/v4/i2/2.ISCA-RJCS-2013-181.php>
- ²⁸ I. D. Mall, V. C. Srivastava, N. K. Agarwal and I. M. Mishra, *Chemosphere*, **61**, 492 (2005), <https://doi.org/10.1016/j.chemosphere.2005.03.065>

- ²⁹ D. Ozer, G. Dursun and A. Ozer, *J. Hazard. Mater.*, **144**, 171 (2007), <https://doi.org/10.1016/j.jhazmat.2006.09.092>
- ³⁰ J. Song, W. Zou, Y. Bian, F. Su and R. Han, *Desalination*, **265**, 119 (2011), <https://doi.org/10.1016/j.desal.2010.07.041>
- ³¹ A. W. Krowiak, R. G. Szafran and S. Modelski, *Desalination*, **265**, 126 (2011), <https://doi.org/10.1016/j.desal.2010.07.042>
- ³² Q. Li, J. Zhai, W. Zhang, M. Wang and J. Zhou, *J. Hazard. Mater.*, **141**, 163 (2007), <https://doi.org/10.1016/j.jhazmat.2006.06.109>
- ³³ S. Zhang, R. Zhang, W. Xiao and R. Han, *Water Sci. Technol.*, **68**, 2158 (2013), <https://doi.org/10.2166/wst.2013.464>
- ³⁴ D. Ranjbar, M. Raeeszadeh, L. Lewis, M. J. MacLachlan and S. G. Hatzikiriakos, *Cellulose*, **27**, 3211 (2020), <https://doi.org/10.1007/s10570-020-03021-z>
- ³⁵ M. M. Rahman, N. Akter, M. R. Karim, N. Ahmad, M. M. Rahman *et al.*, *J. Environ. Chem. Eng.*, **2**, 76 (2014), <https://doi.org/10.1016/j.jece.2013.11.023>
- ³⁶ T. K. Saha, N. C. Bhoumik, S. Karmaker, M. G. Ahmed, H. Ichikawa *et al.*, *Clean-Soil, Air, Water*, **39**, 984 (2011), <https://doi.org/10.1002/clen.201000315>
- ³⁷ S. Karmaker, T. Sen and T. K. Saha, *Polym. Bull.*, **72**, 1879 (2015), <https://doi.org/10.1007/s00289-015-1378-4>
- ³⁸ S. N. Jain, S. R. Tamboli, D. S. Sutar, S. R. Jadhav, J. V. Marathe *et al.*, *Biomass Conv. Bioref.*, (2020), <https://doi.org/10.1007/s13399-020-00780-4>
- ³⁹ S. Lagergren, *K. Sven. Vetenskapsakad Handl.*, **24**, 1 (1898)
- ⁴⁰ Y. S. Ho and G. McKay, *Process Biochem.*, **34**, 451 (1999), [https://doi.org/10.1016/S0032-9592\(98\)00112-5](https://doi.org/10.1016/S0032-9592(98)00112-5)
- ⁴¹ S. Y. Elovich and O. G. Larinov, *Izv. Akad. Nauk. SSSR, Otd. Khim. Nauk*, **2**, 209 (1962)
- ⁴² G. E. Boyd, A. W. Adamson and Jr. L. S. Myers, *J. Am. Chem. Soc.*, **69**, 2836 (1947), <https://doi.org/10.1021/ja01203a066>
- ⁴³ W. J. Weber and J. C. Morris, *J. Sanit. Eng. Div. Proc. Am. Soc. Civ. Eng.*, **89**, 31 (1963), <https://doi.org/10.1061/JSEDAI.0000430>
- ⁴⁴ A. Abdelhay, A. A. Bsoul, A. Al-Othman, N. M. Al-Ananzeh, I. Jum'h *et al.*, *Adsorp. Sci. Technol.*, **36**, 46 (2018), <https://doi.org/10.1177/0263617416684347>
- ⁴⁵ Y. S. Ho and G. McKay, *Chem. Eng. J.*, **70**, 115 (1998), [https://doi.org/10.1016/S0923-0467\(98\)00076-1](https://doi.org/10.1016/S0923-0467(98)00076-1)
- ⁴⁶ C. H. Wu, *J. Hazard. Mater.*, **144**, 93 (2007), <https://doi.org/10.1016/j.jhazmat.2006.09.083>
- ⁴⁷ P. D. Petrolekas and G. Maggenakis, *Ind. Eng. Chem. Res.*, **46**, 1326 (2007), <https://doi.org/10.1021/ie061222u>
- ⁴⁸ M. Miyahara and M. Okazaki, *J. Chem. Eng. Jpn.*, **26**, 510 (1993), <https://doi.org/10.1252/jcej.26.510>
- ⁴⁹ E. Eren, *Clean-Soil, Air, Water*, **38**, 758 (2010), <https://doi.org/10.1002/clen.201000060>
- ⁵⁰ S. Karmaker, F. Sintaha and T. K. Saha, *Adv. Biol. Chem.*, **9**, 1 (2019), <https://doi.org/10.4236/abc.2019.91001>
- ⁵¹ H. M. F. Freundlich, *Z. Phys. Chem.*, **57**, 385 (1906), <https://doi.org/10.1515/zpch-1907-5723>
- ⁵² M. I. Temkin and V. Pyzhev, *Acta Physicochim. URSS*, **12**, 217 (1940)
- ⁵³ I. Langmuir, *J. Am. Chem. Soc.*, **40**, 1361 (1918), <https://doi.org/10.1021/ja02242a004>
- ⁵⁴ Y. Liu, *Colloids Surf., A* **274**, 34 (2006), <https://doi.org/10.1016/j.colsurfa.2005.08.029>